Electronic Supplementary Material (ESI) for Journal of Materials Chemistry C

Supporting Information

Synthesis, optical properties and charge transport characteristics of a series of novel thiophene-fused phenazine derivatives

Yongfa Xie,[a] Takuya Fujimoto,[a] Simon Dalgleish,[a] Yoshiaki Shuku,[a] Michio M. Matsushita*[a] and Kunio Awaga*[a,b]

[a] *Department of Chemistry & Research Center for Material Science, Nagoya University, Furo-cho, Chikusa-ku, Nagoya 464-8602, Japan. E-mail: mmmatsushita@nagoya-u.jp, Awaga@mbox.chem.nagoya-u.ac.jp*
[b] *CREST, JST, Furo-cho, Chikusa-ku, Nagoya 464-8602, Japan.*

Contents

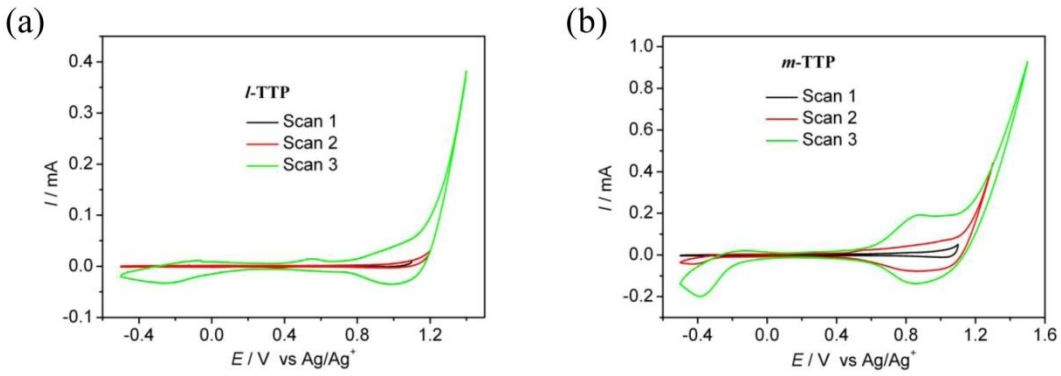

Figure S1. Cyclic voltammograms (scan rate 100 mV s^{-1}) of 100nm thin film of ***l*-TTP** and ***m*-TTP** on ITO recorded in DCM solution containing (n-Bu_4N)PF_6 (0.1M) as electrolyte. ITO and a Pt electrode were used for the working electrode and the counter electrode, respectively. Potentials referenced to Ag/Ag^+.

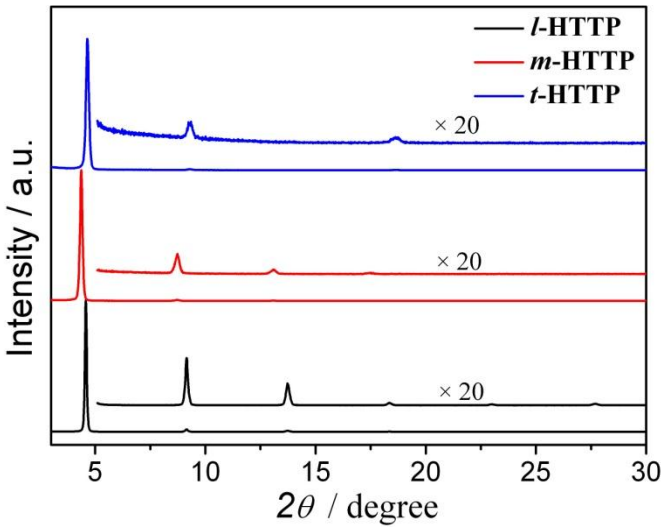

Figure S2. Out-of-plane XRD pattern of ***l*-HTTP**, ***t*-HTTP** and ***m*-HTTP** vacuum-sublimed on Si substrates (no peak in in-plane spectrum) with T_{sub} = 75˚C.

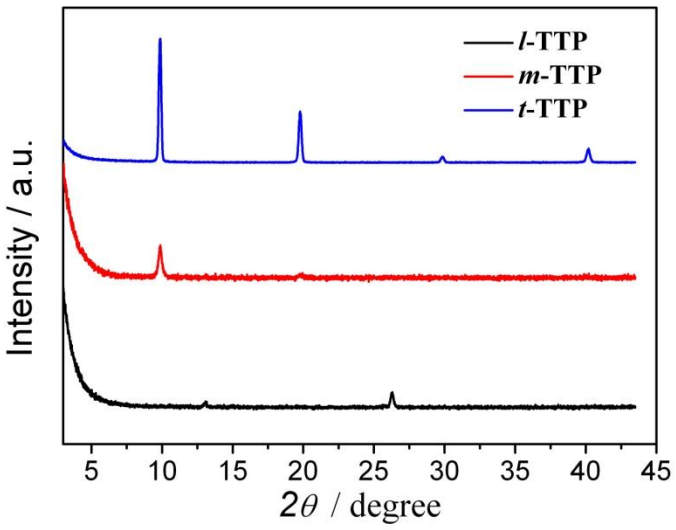

Figure S3. Out-of-plane XRD pattern (Cu $K\alpha$ source: λ = 1.541 Å) of ***l*-TTP**, ***m*-TTP** and ***t*-TTP** vacuum-sublimed on Si substrates (no peak in in-plane spectrum) at T_{sub} = 25 ℃.

Table S1. Absorption wavelengths and their theoretical assignments for *l*-TTP, *m*-TTP, *t*-TTP, *l*-TTA, and *t*-TTA.

	Observed absorption band (λ_{max})	Calculated by TD-DFT	Assigned transition[a]	Energy difference	Contri-bution	Oscillator strength (*f*)
***l*-TTP**	302 nm	286 nm	HOMO→LUMO + 2	4.56 eV	0.24	0.831
			HOMO - 2→LUMO	3.74 eV	0.64	
	408 nm	375 nm	HOMO→LUMO + 2	4.56 eV	0.62	0.399
			HOMO - 2→LUMO	3.74 eV	-0.16	
***m*-TTP**	312 nm	309 nm	HOMO→LUMO + 1	4.42 eV	0.58	0.381
			HOMO - 1→LUMO	3.50 eV	-0.12	
	439 nm	405 nm	HOMO→LUMO + 1	4.42 eV	0.22	0.325
			HOMO - 1→LUMO	3.50 eV	0.64	
***t*-TTP**	320 nm	311 nm	HOMO - 1→LUMO + 1	4.37 eV	0.63	0.797
			HOMO→LUMO	3.29 eV	0.13	
	467 nm	432 nm	HOMO - 1→LUMO + 1	4.37 eV	-0.22	0.302
			HOMO→LUMO	3.29 eV	0.64	
***l*-TTA**	300 nm (strong)	286 nm	HOMO→LUMO + 2	4.63 eV	0.59	1.446
			HOMO - 1→LUMO	4.13 eV	0.35	
	479 nm (weak)	350 nm	HOMO→LUMO + 2	4.63 eV	-0.35	0.127
			HOMO - 1→LUMO	4.13 eV	0.61	
***t*-TTA**	310 nm (strong)	320 nm	HOMO→LUMO + 1	4.09 eV	0.60	1.262
			HOMO - 1→LUMO	3.77 eV	-0.37	
	418 nm (weak)	393 nm	HOMO→LUMO + 1	4.09 eV	0.37	0.058
			HOMO - 1→LUMO	3.77 eV	0.60	

[a] Assigned transitions and their corresponding energy difference were showed in Figure 4.

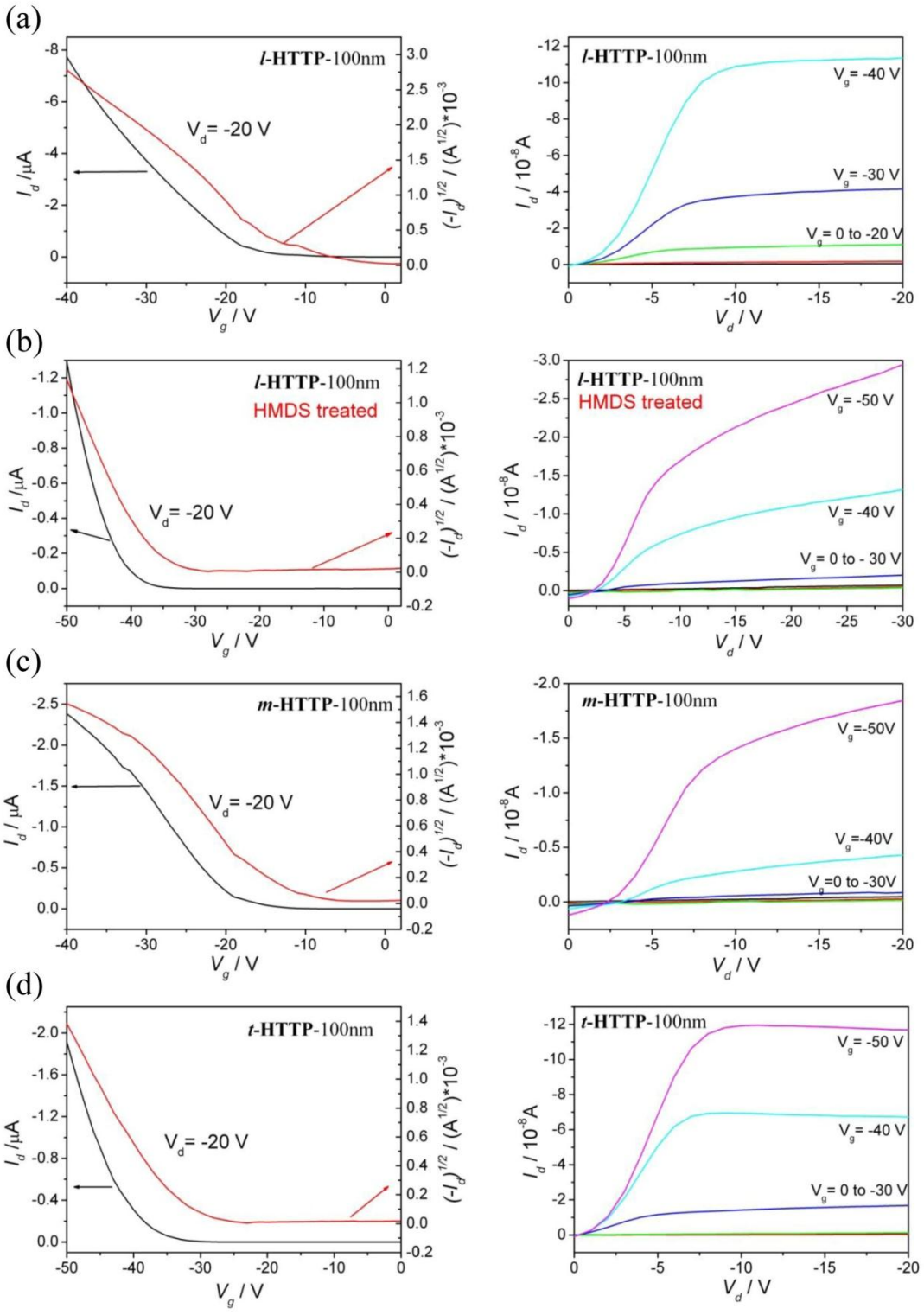

Figure S4. Transfer (left) and output (right) characteristics of thin films of ***l*-HTTP** (a), ***m*-HTTP** (c) and ***t*-HTTP** (d) vacuum-sublimed on SiO_2/Si. Thin film of ***l*-HTTP** on HMDS treated SiO_2/Si (b).

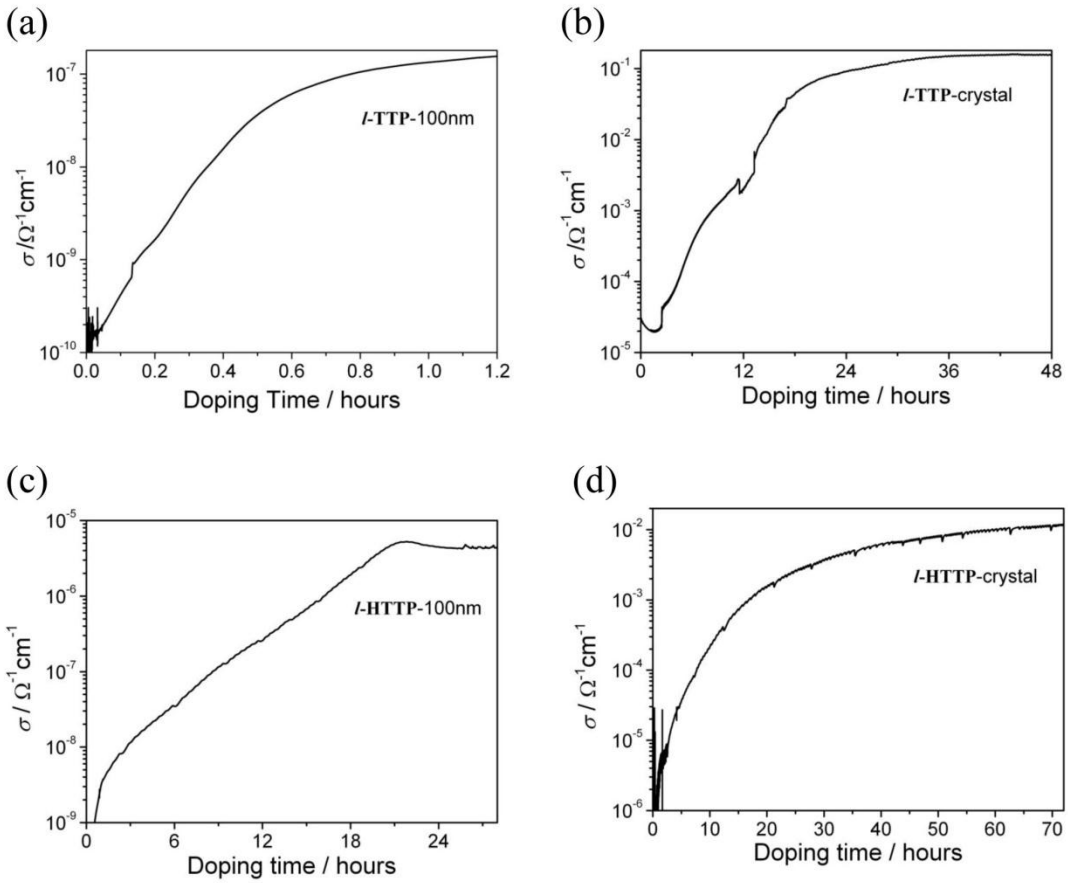

Figure S5. Conductivity change during I_2 vapor doping in thin film (a) and crystal (b) of ***l*-TTP**; and thin film (c) and crystal (d) of ***l*-HTTP** (conductivity data of the other derivatives are listed in Table 4).

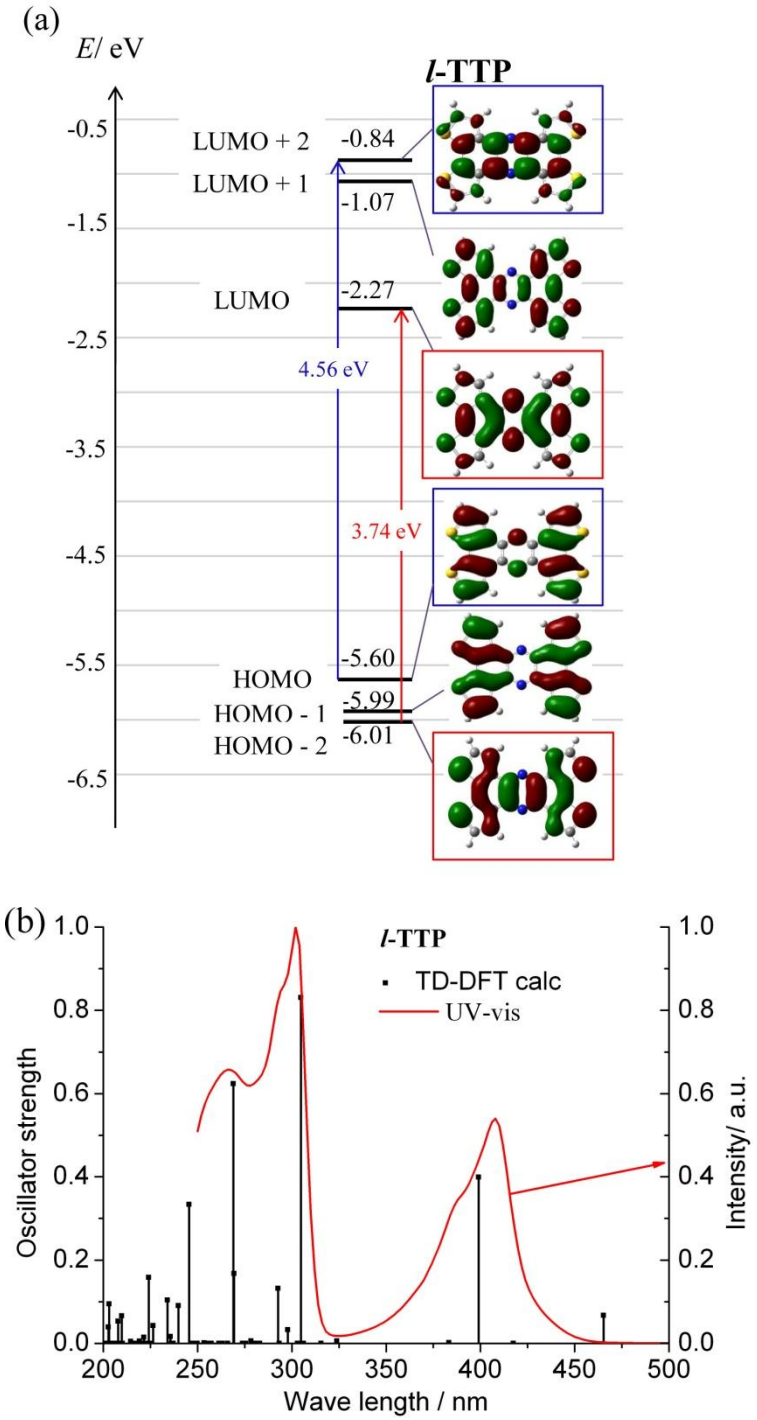

Observed absorption band (λ_{max})	Calculated by TD-DFT	Assigned transition	Energy difference	Contribution	Oscillator strength (*f*)
302 nm	286 nm	HOMO→LUMO + 2	4.56 eV	0.24	0.831
		HOMO - 2→LUMO	3.74 eV	0.64	
408 nm	375 nm	HOMO→LUMO + 2	4.56 eV	0.62	0.399
		HOMO - 2→LUMO	3.74 eV	-0.16	

Figure S6. (a) Energy diagram and distributions of frontier orbitals of ***l*-TTP** accompanied with the assignment of optical transitions. (b) UV-vis spectrum of ***l*-TTP** (red line) in $CHCl_3$ accompanied with a simulated transitions (black line) calculated by TD-DFT method (B3LYP/6-31G (d)). Scalling factor is 0.94.

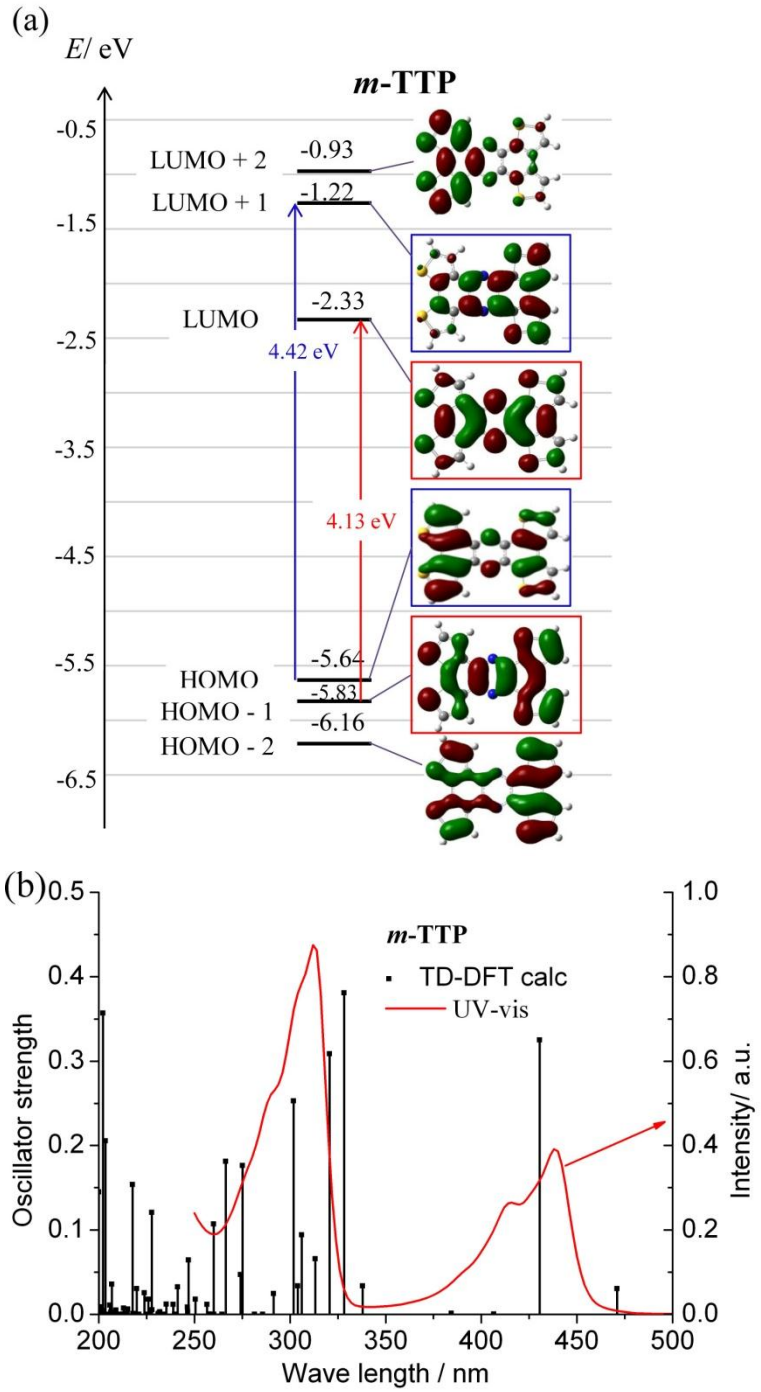

Observed absorption band (λ_{max})	Calculated by TD-DFT	Assigned transition	Energy difference	Contribution	Oscillator strength (f)
312 nm	309 nm	HOMO→LUMO + 1	4.42 eV	0.58	0.381
		HOMO - 1→LUMO	4.13 eV	-0.12	
439 nm	405 nm	HOMO→LUMO + 1	4.42 eV	0.22	0.325
		HOMO - 1→LUMO	4.13 eV	0.64	

Figure S7. (a) Energy diagram and distributions of frontier orbitals of ***m*-TTP** accompanied with the assignment of optical transitions. (b) UV-vis spectrum of ***m*-TTP** (red line) in $CHCl_3$ accompanied with a simulated transitions (black line) calculated by TD-DFT method (B3LYP/6-31G (d)). Scalling factor is 0.94.

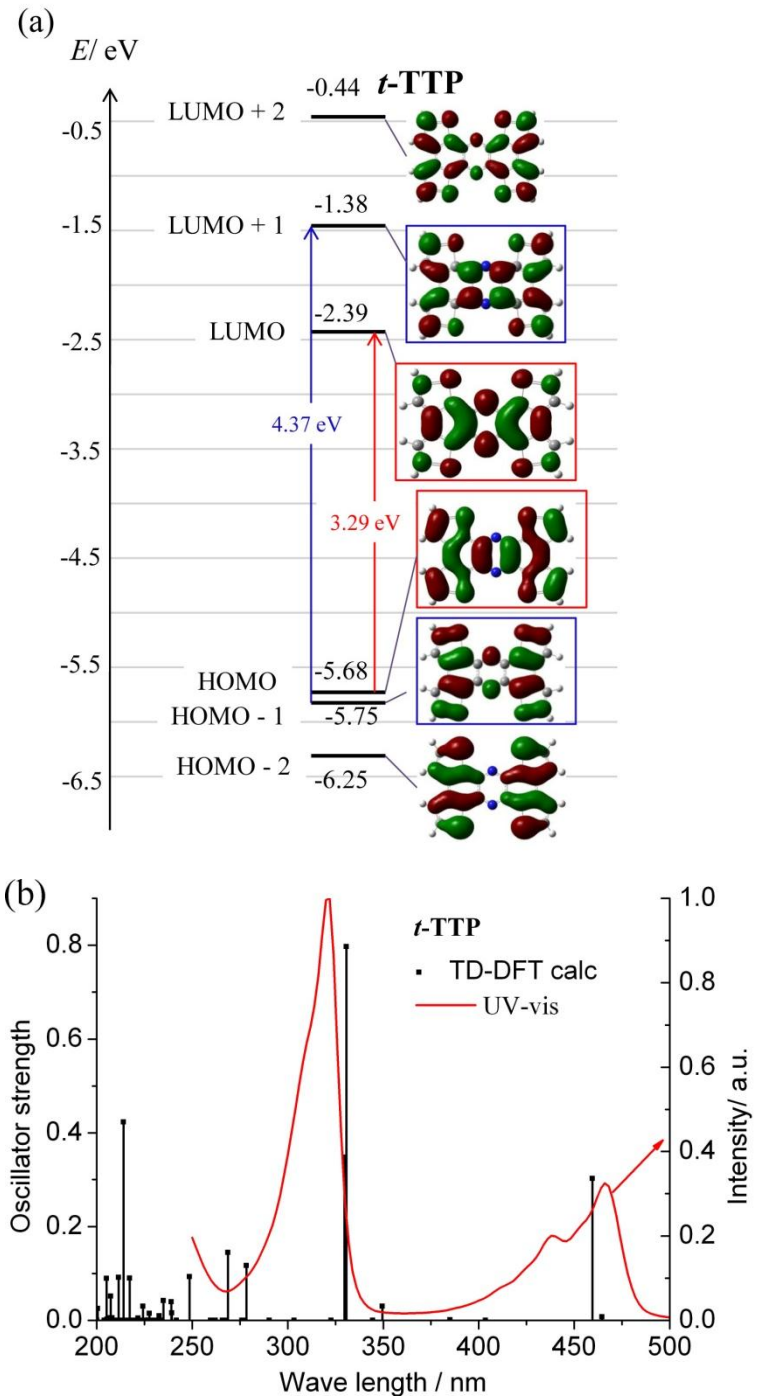

Observed absorption band (λ_{max})	Calculated by TD-DFT	Assigned transition	Energy difference	Contribution	Oscillator strength (f)
320 nm	311 nm	HOMO - 1→LUMO + 1	4.37 eV	0.63	0.797
		HOMO→LUMO	3.29 eV	0.13	
467 nm	432 nm	HOMO - 1→LUMO + 1	4.37 eV	-0.22	0.302
		HOMO→LUMO	3.29 eV	0.64	

Figure S8. *t*-TTP: (a) Energy diagram and distributions of frontier orbitals of ***t*-TTP** accompanied with the assignment of optical transitions. (b) UV-vis spectrum of ***t*-TTP** (red line) in $CHCl_3$ accompanied with a simulated transitions (black line) calculated by TD-DFT method (B3LYP/6-31G (d)). Scalling factor is 0.94.

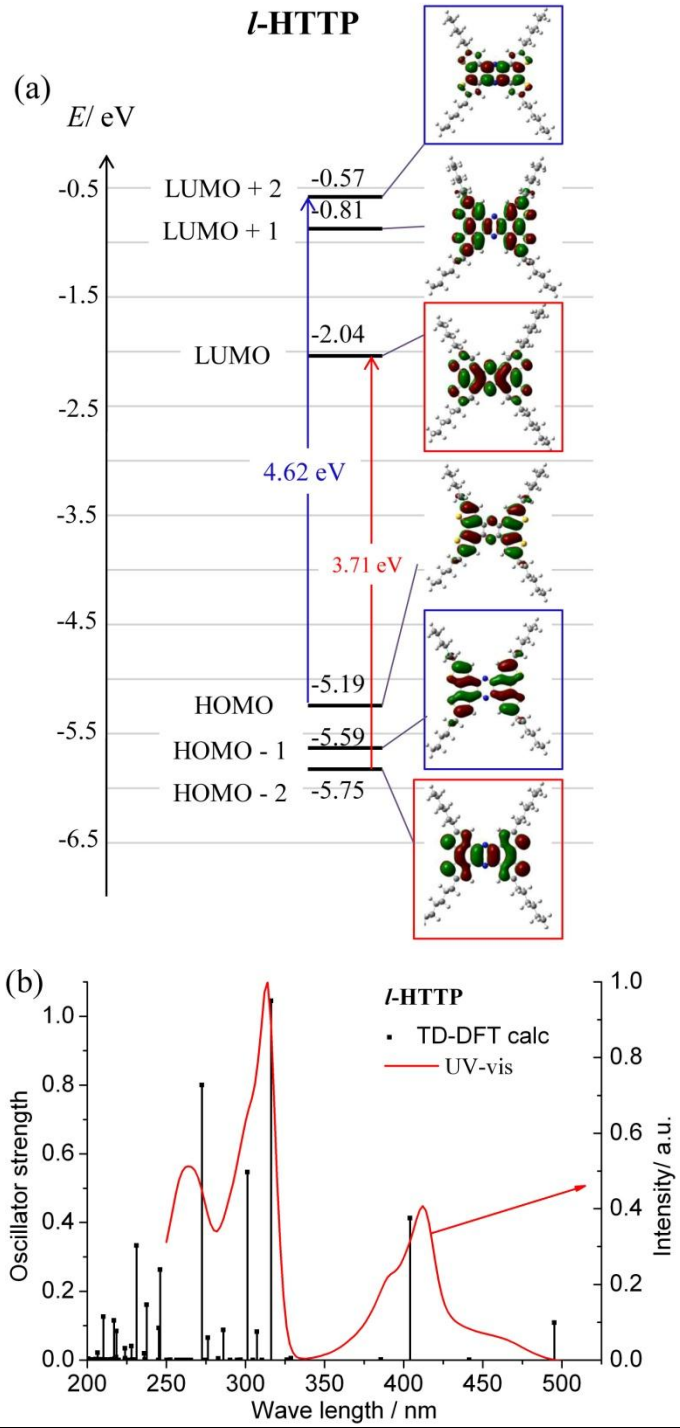

Observed absorption band (λ_{max})	Calculated by TD-DFT	Assigned transition	Energy difference	Contribution	Oscillator strength (f)
313 nm	296 nm	HOMO→LUMO + 2	4.62 eV	0.61	0.900
		HOMO - 2→LUMO	3.71 eV	0.17	
422 nm	380 nm	HOMO→LUMO + 2	4.62 eV	-0.25	0.378
		HOMO - 2→LUMO	3.71 eV	0.64	

Figure S9. (a) Energy diagram and distributions of frontier orbitals of ***l*-HTTP** accompanied with the assignment of optical transitions. (b) UV-vis spectrum of ***l*-HTTP** (red line) in $CHCl_3$ accompanied with a simulated transitions (black line) calculated by TD-DFT method (B3LYP/6-31G (d)). Scalling factor is 0.94.

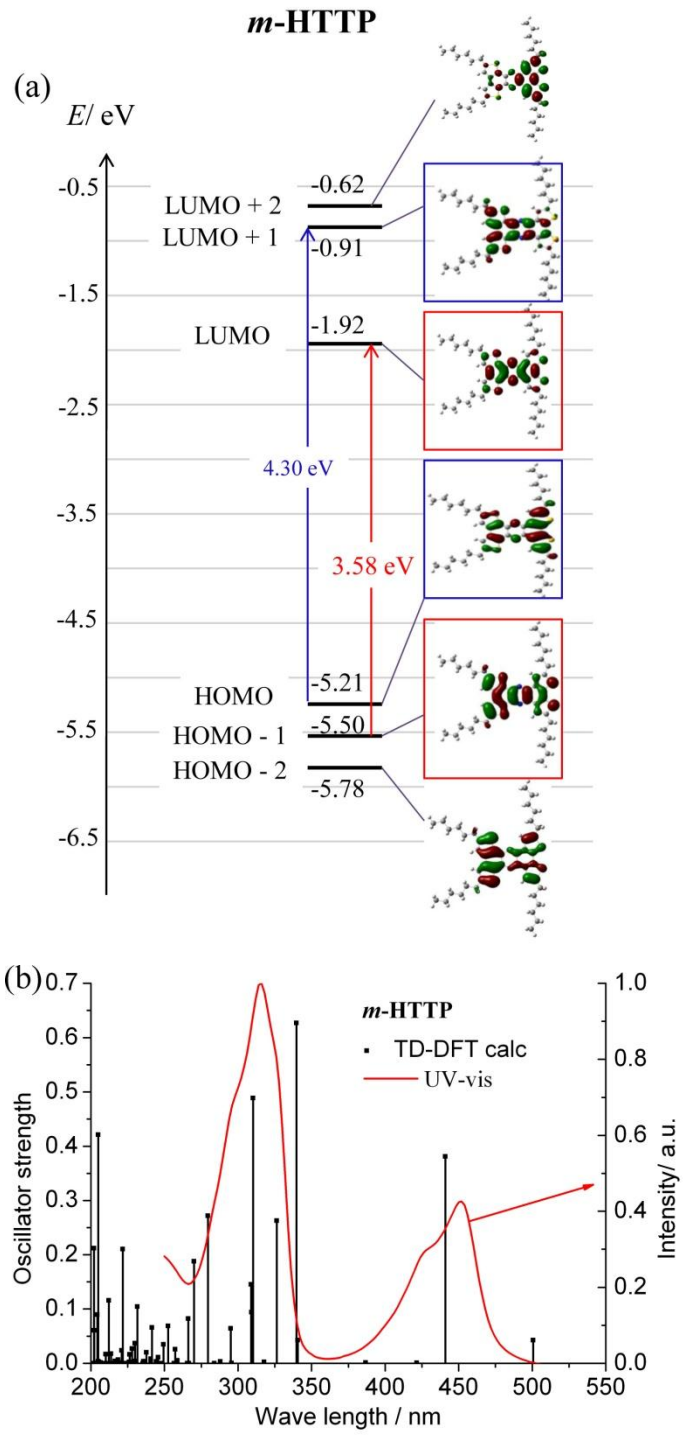

Observed absorption band (λ_{max})	Calculated by TD-DFT	Assigned transition	Energy difference	Contribution	Oscillator strength (*f*)
315 nm	319 nm	HOMO→LUMO + 1	4.30 eV	0.62	0.627
		HOMO - 1→LUMO	3.58 eV	0.13	
451 nm	414 nm	HOMO→LUMO + 1	4.30 eV	-0.21	0.381
		HOMO - 1→LUMO	3.58 eV	0.64	

Figure S10. (a) Energy diagram and distributions of frontier orbitals of ***m*-HTTP** accompanied with the assignment of optical transitions. (b) UV-vis spectrum of ***m*-HTTP** (red line) in $CHCl_3$ accompanied with a simulated transitions (black line) calculated by TD-DFT method (B3LYP/6-31G (d)). Scalling factor is 0.94.

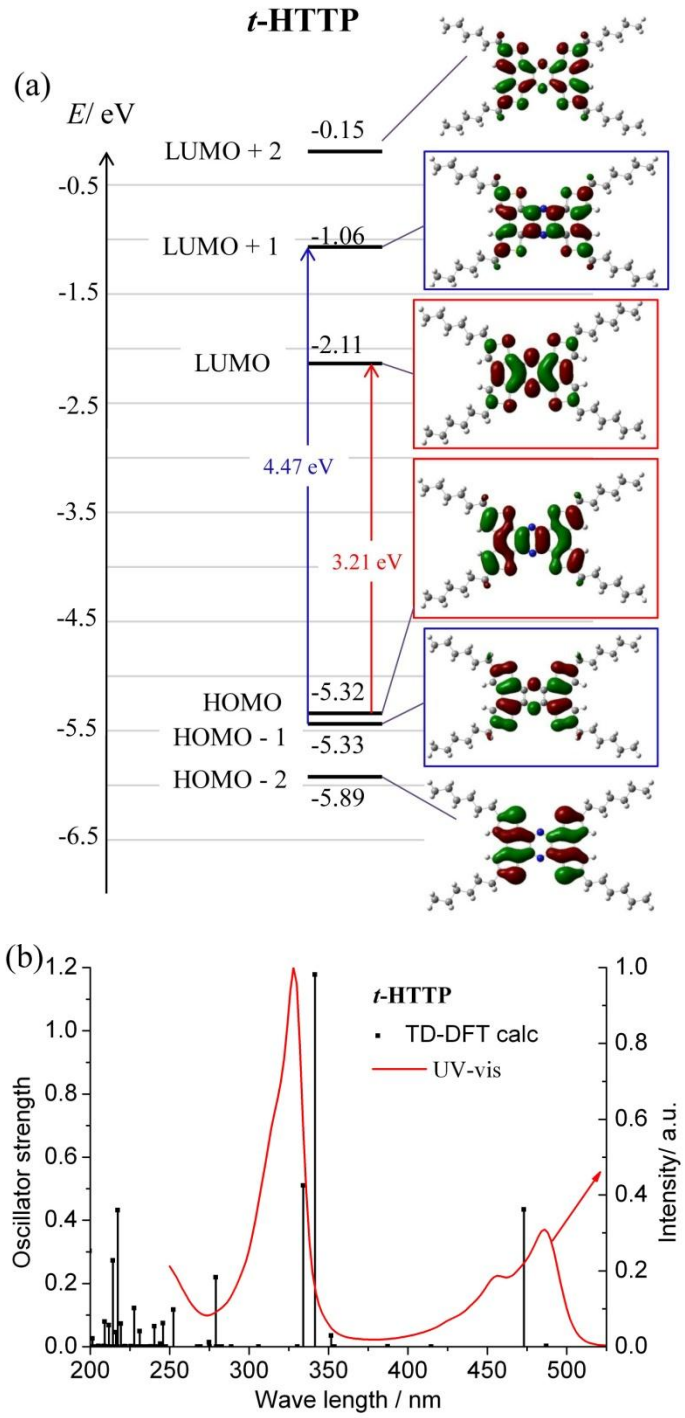

Observed absorption band (λ_{max})	Calculated by TD-DFT	Assigned transition	Energy difference	Contribution	Oscillator strength (*f*)
328 nm	321 nm	HOMO - 1→LUMO + 1	4.47 eV	0.64	1.178
		HOMO→LUMO	3.21 eV	0.13	
486 nm	445 nm	HOMO - 1→LUMO + 1	4.47 eV	-0.21	0.434
		HOMO→LUMO	3.21 eV	0.64	

Figure S11. (a) Energy diagram and distributions of frontier orbitals of ***t*-HTTP** accompanied with the assignment of optical transitions. (b) UV-vis spectrum of ***t*-HTTP** (red line) in $CHCl_3$ accompanied with a simulated transitions (black line) calculated by TD-DFT method (B3LYP/6-31G (d)). Scalling factor is 0.94.

***l*-TTA**

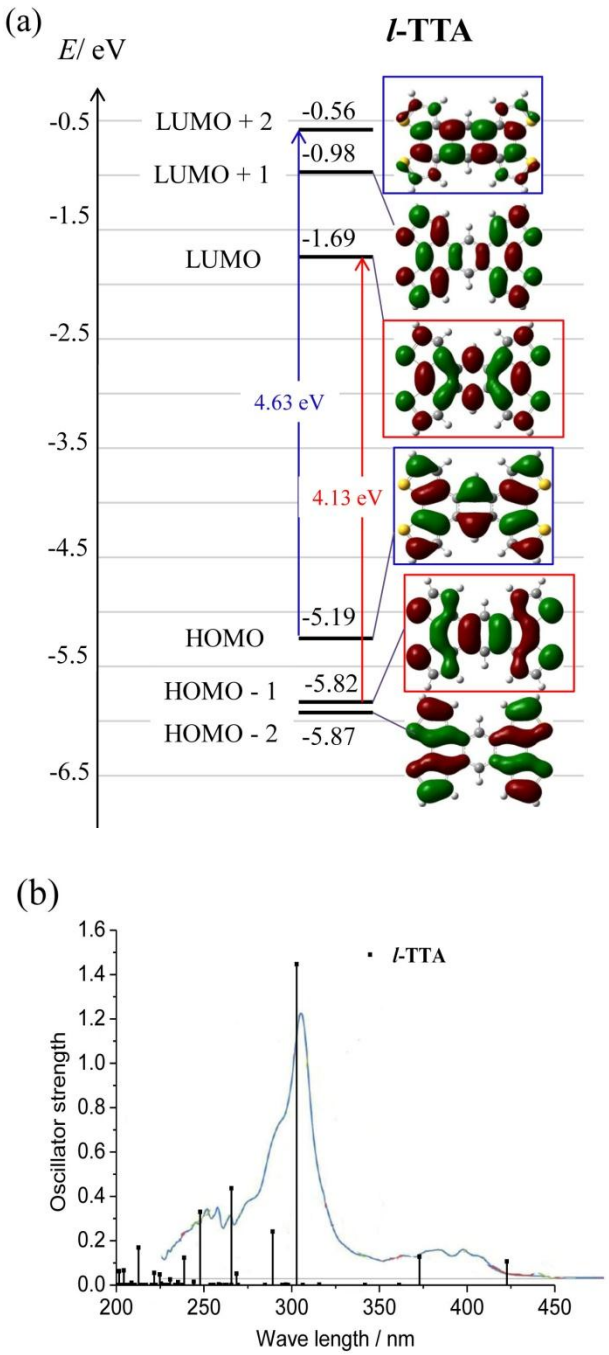

Observed absorption band (λ_{max})	Calculated by TD-DFT	Assigned transition	Energy difference	Contribution	Oscillator strength (*f*)
300 nm(strong)	286 nm	HOMO→LUMO + 2	4.63 eV	0.59	1.446
		HOMO - 1→LUMO	4.13 eV	0.35	
479 nm(weak)	350 nm	HOMO→LUMO + 2	4.63 eV	-0.35	0.127
		HOMO - 1→LUMO	4.13 eV	0.61	

Figure S12. *l*-TTA: (a) Energy diagram and distributions of frontier orbitals of ***l*-TTA** accompanied with the assignment of optical transitions. (b) UV-vis spectrum of ***l*-TTA** (blue line) in DCM[1] accompanied with a simulated transitions (black line) calculated by TD-DFT method (B3LYP/6-31G (d)). Scalling factor is 0.94.

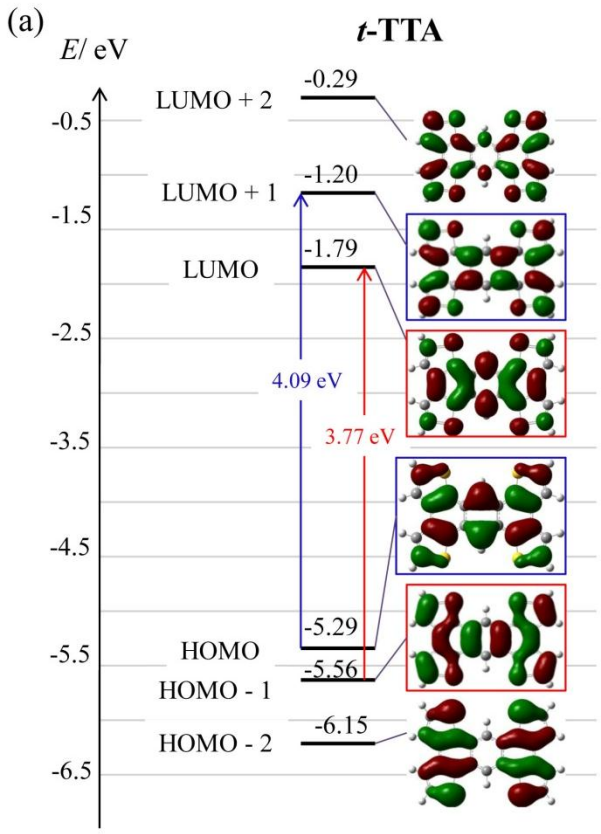

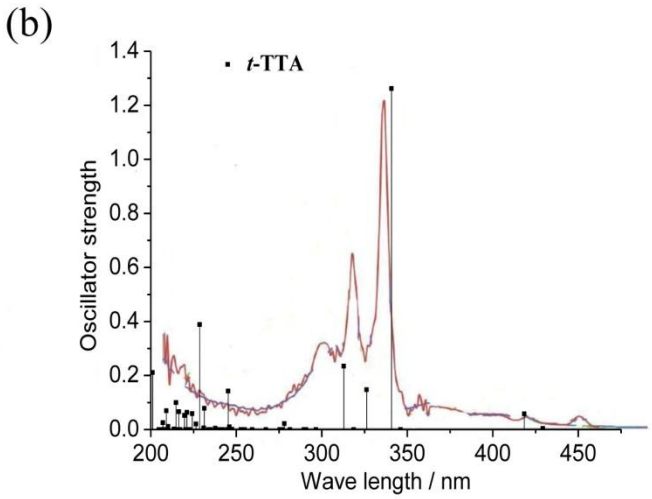

Observed absorption band (λ_{max})	Calculated by TD-DFT	Assigned transition	Energy difference	Contribution	Oscillator strength (f)
310 nm (strong)	320 nm	HOMO→LUMO + 1	4.09 eV	0.60	1.262
		HOMO - 1→LUMO	3.77 eV	-0.37	
418 nm (weak)	393 nm	HOMO→LUMO + 1	4.09 eV	0.37	0.058
		HOMO - 1→LUMO	3.77 eV	0.60	

Figure S13. ***t*-TTA**: (a) Energy diagram and distributions of frontier orbitals of ***t*-TTA** accompanied with the assignment of optical transitions. (b) UV-vis spectrum of ***t*-TTA** (purple line) in DCM[1] accompanied with a simulated transitions (black line) calculated by TD-DFT method (B3LYP/6-31G (d)). Scalling factor is 0.94.

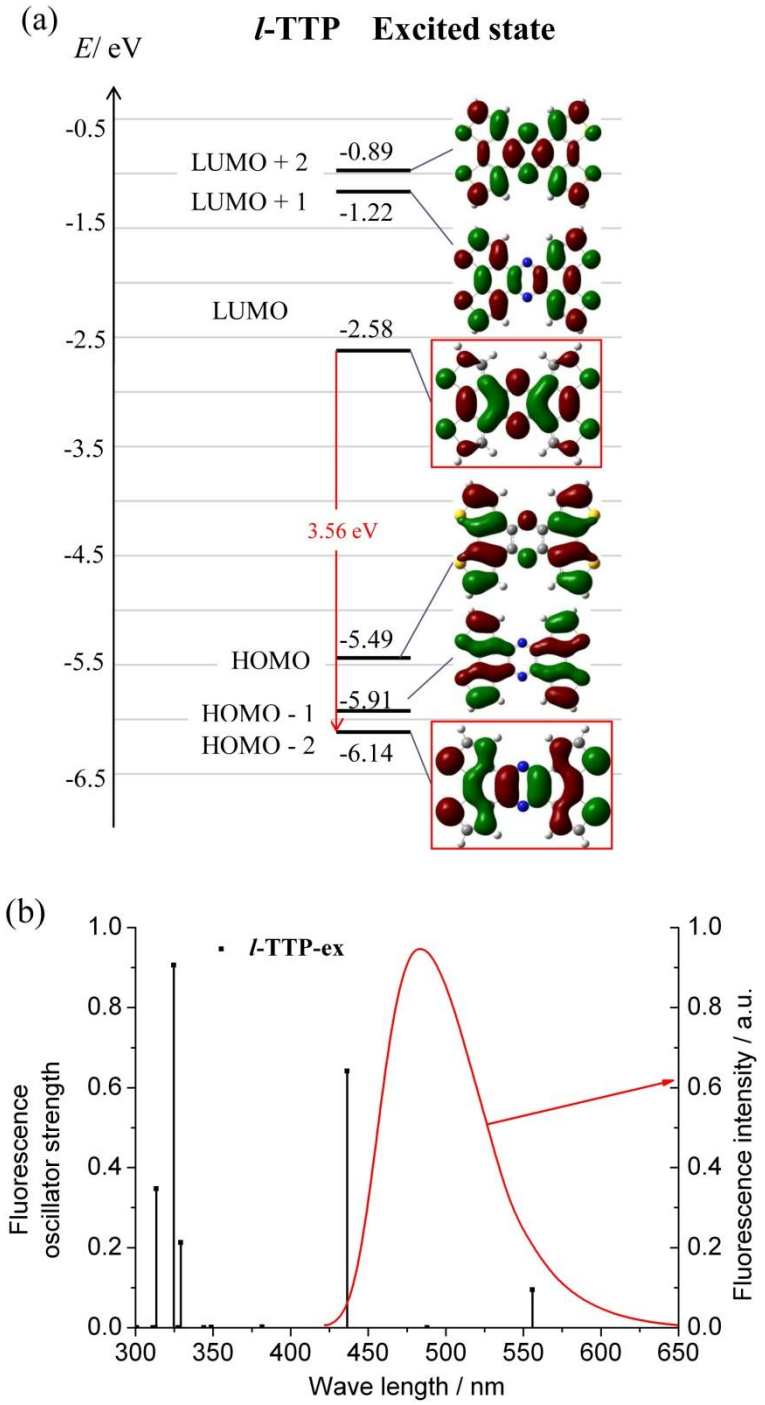

Observed absorption band (λ_{max})	Calculated by TD-DFT	Assigned transition	Energy difference	Contribution	Oscillator strength (*f*)
480 nm	410 nm	LUMO→HOMO - 2	3.56 eV	0.69	0.642
		LUMO + 3→HOMO	---	-0.15	

Figure S14. (a) Energy diagram and spatial distributions of frontier orbitals of an excited state of ***l*-TTP** accompanied with the assignment of photoluminescence transition. (b) Observed fluorescence spectrum (red line) of in $CHCl_3$ solution (λ_{ex} = 303 nm) and simulated spectrum (black line) with TD-DFT method (B3LYP/6-31G (d)). Scalling factor is 0.94.

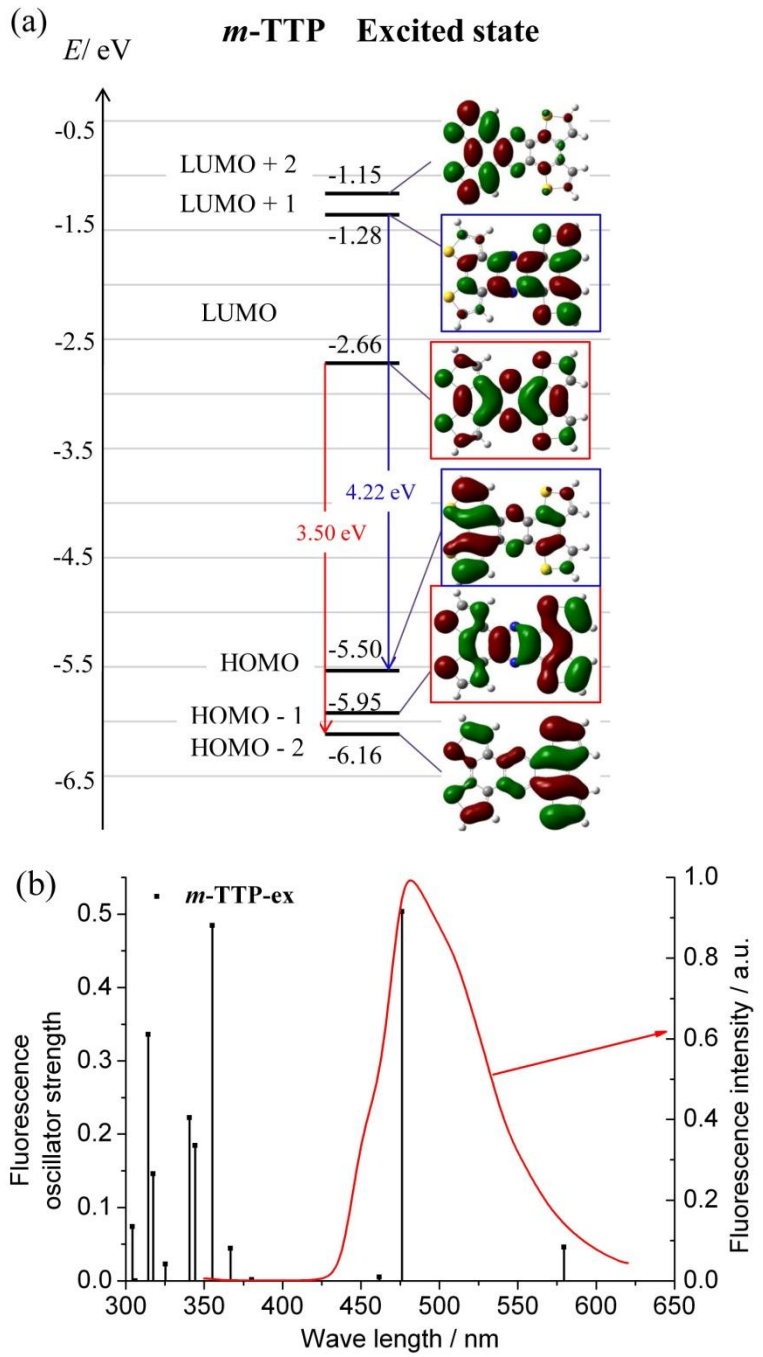

Observed absorption band (λ_{max})	Calculated by TD-DFT	Assigned transition	Energy difference	Contribution	Oscillator strength (f)
481 nm	448 nm	LUMO→HOMO - 1	3.50 eV	0.69	0.503
		LUMO + 1→HOMO	4.22 eV	-0.12	

Figure S15. (a) Energy diagram and spatial distributions of frontier orbitals of an excited state of ***m*-TTP** accompanied with the assignment of photoluminescence transition. (b) Observed fluorescence spectrum (red line) of in $CHCl_3$ solution (λ_{ex} = 316 nm) and simulated spectrum (black line) with TD-DFT method (B3LYP/6-31G (d)). Scalling factor is 0.94.

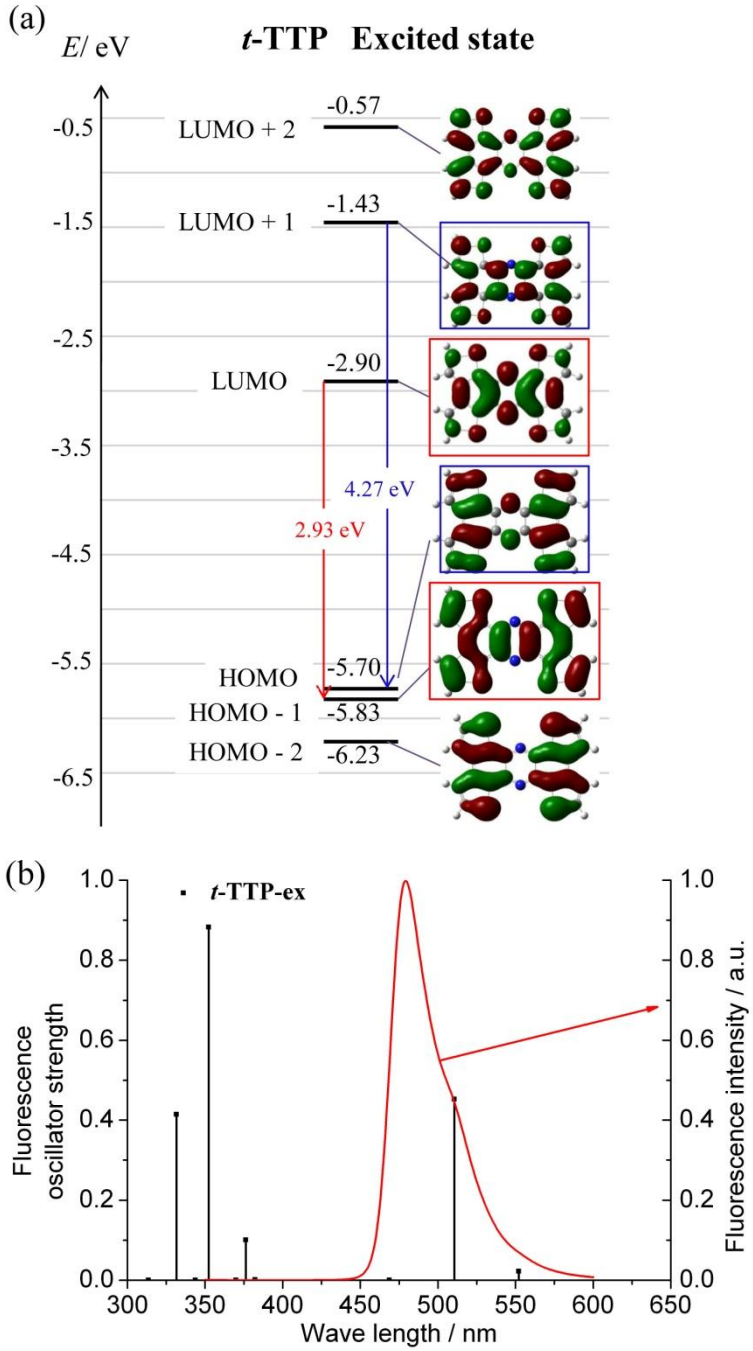

Observed absorption band (λ_{max})	Calculated by TD-DFT	Assigned transition	Energy difference	Contribution	Oscillator strength (*f*)
481 nm	480 nm	LUMO→HOMO - 1	2.93 eV	0.70	0.453
		LUMO + 1→HOMO	4.27 eV	-0.12	

Figure S16. (a) Energy diagram and spatial distributions of frontier orbitals of an excited state of ***t*-TTP** accompanied with the assignment of photoluminescence transition. (b) Observed fluorescence spectrum (red line) of in $CHCl_3$ solution (λ_{ex} = 322 nm) and simulated spectrum (black line) with TD-DFT method (B3LYP/6-31G (d)). Scalling factor is 0.94.

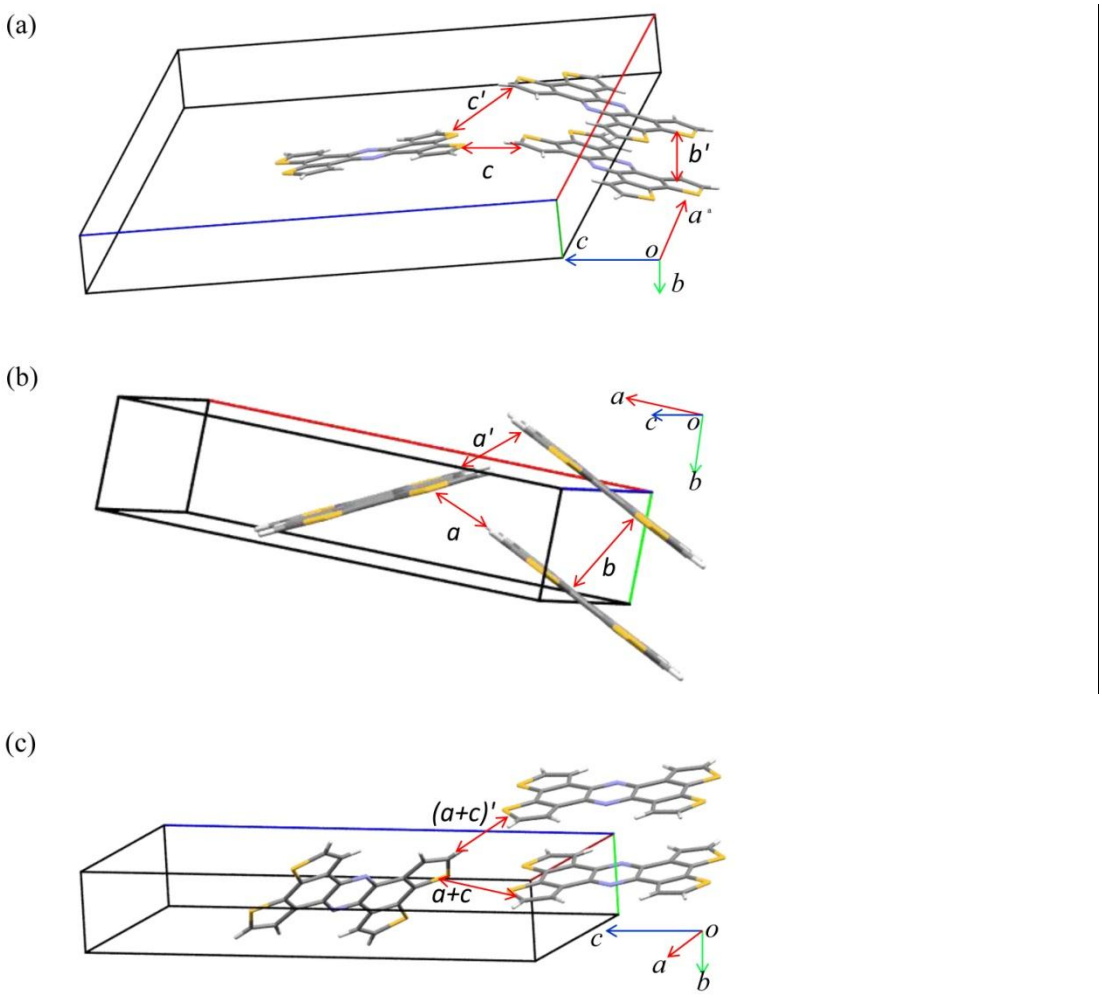

Figure S17. Effective intermolecular contacts in ***l*-TTP** crystal along *b*-axis (a), *b*-axis (b) and a + c direction (c).

Table S2. Theoretical estimated intermolecular transfer intergrals (*Hab*), overlap intergrals (*Sab*), center-to-center distances (*d*), orbital interaction energy (*V*), reorganization energy (λ) and hopping mobilities for each molecular contact.

	Contact[a]	*Hab*[b] /meV	*Sab*[b] /meV	*d* /Å	*V* /meV	λ[c] / meV	$\mu_{hopping}$ / $cm^2\ V^{-1}\ S^{-1}$
***l*-TTP**	*b*	-135.4	11.2	3.892	-76.5	153	5.3×10^{-1}
***l*-TTP**	*a*	7.7	-0.7	8.748	.3.6	153	6.1×10^{-3}
***l*-TTP**	*c*	-8.9	-0.9	13.001	-.4.0	153	1.7×10^{-2}
***l*-TTP**	*c'*	14.47	-1.6	13.002	.5.9	153	3.5×10^{-2}
***l*-TTP**	*a+c*	-1.5	0.2	12.934	-.0.6	153	4.0×10^{-4}
***l*-TTP**	*(a+c)'*	3.2	-0.3	13.507	.1.6	153	2.9×10^{-3}
***l*-TTP**	*b'*	-162.4	13.9	3.892	-.91.3	153	7.6×10^{-1}

[a] Corresponding molecular contacts are indicated in figure S17. [b] Calculated in PW91/TZ2P level. [c] Calculated in B3LYP/6-31G(d) level.

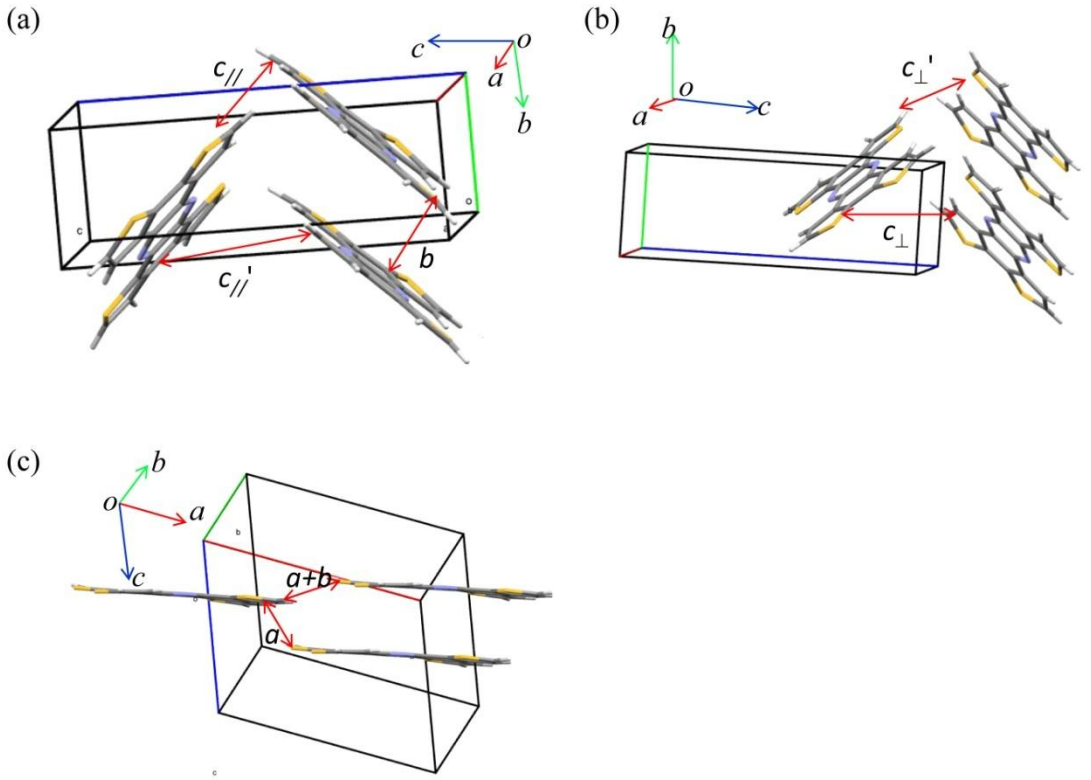

Figure S18. Effective intermolecular contacts in ***m*-TTP** crystal along *c*-axis (a), *a*-axis (b) and a + c direction (c).

Table S3. Theoretical estimated intermolecular transfer intergrals (*Hab*), overlap intergrals (*Sab*), center-to-center distances (*d*), orbital interaction energy (*V*), reorganization energy (λ) and hopping mobilities for each molecular contact.

	Contact[a]	*Hab*[b] /meV	*Sab*[b] /meV	*d* /Å	*V* /meV	λ[c] / meV	$\mu_{hopping}$ / $cm^2\ V^{-1}\ S^{-1}$
***m*-TTP**	*a*	-0.7	0.1	12.581	-0.3	169	8.9×10^{-5}
***m*-TTP**	*a*+*b*	0.4	0	13.474	0.2	169	4.0×10^{-5}
***m*-TTP**	*b*	-133.3	12.9	4.825	-66.5	169	5.0×10^{-1}
***m*-TTP**	$c_{//}$	-1.0	0	7.857	-1.1	169	3.7×10^{-4}
***m*-TTP**	$c_{//}$'	-1.8	0	7.857	-1.9	169	1.1×10^{-3}
***m*-TTP**	$c_{\perp}$	25.9	-2.6	11.941	11.7	169	9.5×10^{-2}
***m*-TTP**	$c_{\perp}$'	25.7	-2.7	11.941	11.5	169	9.2×10^{-2}

[a] Corresponding molecular contacts are indicated in figure S18. [b] Calculated in PW91/TZ2P level. [c] Calculated in B3LYP/6-31G(d) level.

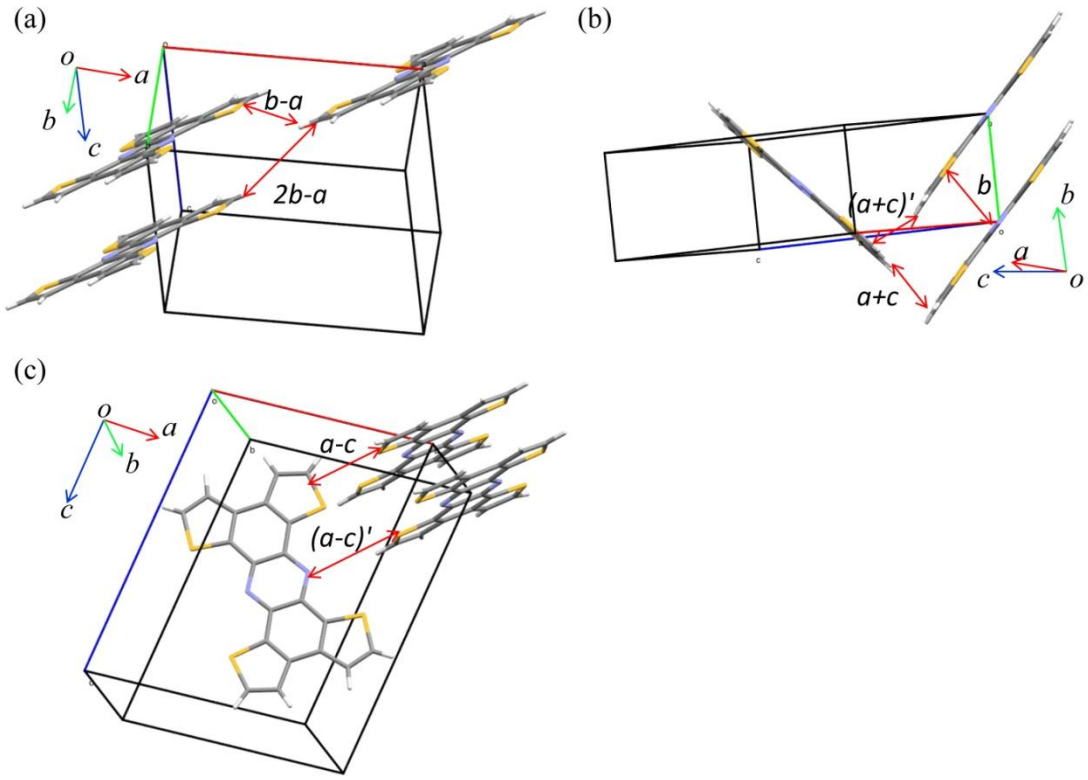

Figure S19. Effective intermolecular contacts in ***t*-TTP** crystal along *c*-axis (a), *b*-axis (b) and a -c direction (c).

Table S4. Theoretical estimated intermolecular transfer intergrals (*Hab*), overlap intergrals (*Sab*), center-to-center distances (*d*), orbital interaction energy (*V*), reorganization energy (λ) and hopping mobilities for each molecular contact.

	Contact[a]	*Hab*[b] /meV	*Sab*[b] /meV	*d* /Å	*V* /meV	λ[c] /m eV	$\mu_{hopping}$ / $cm^2\ V^{-1}\ S^{-1}$
***t*-TTP**	*2b-a*	0.2	-0.02	15.069	0	174	1.9×10^{-6}
***t*-TTP**	*b-a*	0.6	-0.2	12.314	-0.4	174	1.3×10^{-4}
***t*-TTP**	*b*	59.1	-7.4	5.014	20.2	174	4.7×10^{-2}
***t*-TTP**	*a+c*	-21.9	2.4	9.262	-9.3	174	3.4×10^{-2}
***t*-TTP**	*(a+c)'*	-24.1	2.4	9.262	-9.3	174	5.0×10^{-2}
***t*-TTP**	*a-c*	-8.3	0.9	11.862	-3.6	174	8.4×10^{-3}
***t*-TTP**	*(a-c)'*	5.0	-0.4	9.509	3.0	174	3.7×10^{-3}

[a] Corresponding molecular contacts are indicated in figure S19. [b] Calculated in PW91/TZ2P level. [c] Calculated in B3LYP/6-31G(d) level.

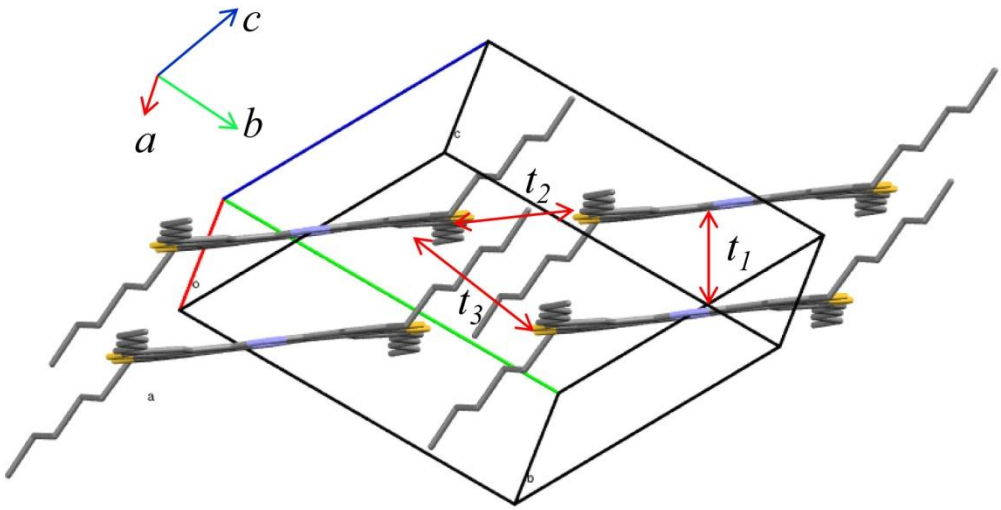

Figure S20. Effective intermolecular contacts in ***l*-HTTP** crystal.

Table S5. Theoretical estimated intermolecular transfer intergrals (*Hab*), overlap intergrals (*Sab*), center-to-center distances (*d*), orbital interaction energy (*V*), reorganization energy (λ) and hopping mobilities for each molecular contact.

	Contact[a]	*Hab*[b] /meV	*Sab*[b] /meV	*d* /Å	*V* /meV	λ[c] /m eV	$\mu_{hopping}$ / $cm^2\ V^{-1}\ S^{-1}$
***l*-HTTP**	t_1	-50.8	5.6	4.892	-25.0	155	8.7×10^{-2}
***l*-HTTP**	t_3	-0.4	0	14.988	0	155	6.3×10^{-5}
***l*-HTTP**	t_2	-3.9	0.4	12.749	-2.0	155	3.8×10^{-3}

[a] Corresponding molecular contacts are indicated in figure S20. [b] Calculated in PW91/TZ2P level. [c] Calculated in B3LYP/6-31G(d) level.

[1] Brusso, J. L.; Hirst, O. D.; Dadvand, A.; Ganesan, S.; Cicoira, F.; Robertson, C. M.; Oakley, R. T.; Rosei, F.; Perepichka, D. F. *Chem. Mater.* **2008**, *20*, 2484-2494.